ACADEMIC
PRESS

Available online at www.sciencedirect.com

SCIENCE DIRECT®

Journal of Catalysis 214 (2003) 146–152

JOURNAL OF
CATALYSIS

www.elsevier.com/locate/jcat

Synthesis and structural characterization of Pt/amorphous Al_2O_3 catalyst

Alon Dolev, Gennady E. Shter, and Gideon S. Grader *

Chemical Engineering Department, Technion, Haifa 32000, Israel

Received 14 June 2002; revised 2 September 2002; accepted 16 September 2002

Abstract

The synthesis of Pt supported on nonhydrolytic derived amorphous alumina catalyst was studied. The Pt was introduced both by in situ gelation with the alumina precursor and by impregnation of the amorphous alumina matrix. The in situ precursors were $PtBr_4$ and $(C_6H_5CN)_2PtCl_2$, while the impregnation precursors were H_2PtCl_6 solution in water and $Pt(acac)_2$ solution in toluene. For comparison, samples of commercial γ-Al_2O_3 were impregnated by the same methods. Complete fixation of the Pt precursor from the solution to the amorphous alumina support was achieved for both impregnation methods. After 773 K calcination in air the Pt dispersion, determined by H_2 pulse chemisorption, for the in situ gelation-based catalysts was 32%. The corresponding Pt dispersion of the impregnated catalysts, prepared with H_2PtCl_6 and $Pt(acac)_2$, was 15 and 49%, respectively. The low dispersion obtained using H_2PtCl_6 solution in water is explained by the partial burial of the Pt by a dissolution reprecipitation of the amorphous alumina and by a condensation reaction which occurs upon contact with water. These processes also cause reduction in the surface area of the amorphous alumina upon subsequent calcination.

Keywords: Amorphous; Alumina; Nonhydrolytic; Pt; Catalyst; Synthesis; Characterization; Dispersion; Impregnation; Gelation

1. Introduction

Porous aluminas with large surface areas (SA) are widely used in catalytic applications. In applications as isomerization, hydrocracking, cyclization, and dehydration the alumina serves as a bifunctional carrier or as the catalyst itself and therefore the acidic sites on the alumina play a major role in the catalytic activity [1]. The most common alumina supports are γ and η phases, and the main route to obtaining large SA aluminas is the hydrolytic sol–gel process [2,3].

In the past decade a new route for the production of transition metal oxides by a nonhydrolytic (NH) sol–gel process was developed [4–11]. The NH alumina retains high SA and is in the amorphous state up to 1073–1123 K. Additionally, the NH alumina also retains ~ 2 wt.% Cl up to the crystallization temperature. For applications such as naphtha reforming Cl is added in order to enhance the acidic function of the alumina [12–14]. Therefore the NH alumina is a promising candidate as a bifunctional support for applications such as hydrocarbon reforming. Moreover, the utilization of this type of NH alumina as a catalyst support has never been examined before.

Pt/Al_2O_3 catalysts, with additional promoters to tune the catalytic activity, are common in applications such as naphtha reforming [14]. These catalysts are also common in automobile catalytic converters. Utilization of amorphous alumina for catalytic applications is very scarce and little has been published regarding the synthesis of amorphous Al_2O_3 and its utilization for catalytic applications. Although the Pt/Al_2O_3 catalyst system has been studied extensively, we found only one work dealing with Pt supported on amorphous Al_2O_3 [15]. In that work the amorphous alumina was impregnated by a methanolic solution of H_2PtCl_6; the obtained catalyst was used to study the spillover of hydrogen and oxygen onto amorphous alumina and was not characterized.

The most common route for the introduction of Pt into porous alumina is by impregnation with an aqueous solution of H_2PtCl_6 precursor. Although the attachment mechanism of the Pt precursor is not clear [16–21], the Pt precursor is fixed to the alumina at discrete sites and therefore is initially dispersed at the atomic level. Contact of the NH-amorphous alumina with water causes morphology changes in the NH alumina matrix [22,23]. It was found that the amorphous alumina may undergo crystallization into pseudo-bohemite, depending on water contact conditions, and upon further calcination the aluminas may undergo crystallization into

---

[*] Corresponding author.
E-mail address: grader@tx.technion.ac.il (G.S. Grader).

0021-9517/03/$ – see front matter © 2003 Elsevier Science (USA). All rights reserved.
doi:10.1016/S0021-9517(02)00022-2

γ-Al_2O_3 in the range 673–773 K. The SA of the alumina after the second calcination also differs from the initial SA of the amorphous alumina. Immersion in water at room temperature (RT) for up to several days causes a decrease in final SA, whereas longer immersion periods result in increased final SA. An alternative route to obtaining well-dispersed Pt on the alumina is by impregnating the alumina with a solution of platinum acetylacetonate [Pt(acac)$_2$] in organic solvents such as toluene or benzene [24–32]. This chlorine-free ligand exchange method does not contribute any additional acidity on the alumina carrier (which does occur when chloroplatinic acid precursor is used) and does not involve contact with water. Yet another approach for the introduction of the noble metal into the support is by introduction of the metal during the gelation of the support by an adequate precursor [33–40]. This one-step method, pioneered by the group of Gomez and Lopez, may result in reduced metal sintering upon thermal treatment [38,39] and in metal–support interactions which may effect the catalytic activity [33–35]. The main drawback of this approach is that the metal might be buried within the support and therefore be catalytically inactive [38,39].

The objectives of this work were the synthesis of Pt/NH-amorphous Al_2O_3 catalysts by several methods and their characterization. The Pt was introduced either by impregnation of the calcined alumina matrix or by in situ gelation with the alumina precursor. The impregnation solutions were (a) chloroplatinic acid in water and (b) Pt(acac)$_2$ in toluene. For comparison purposes commercial γ-aluminas were also impregnated by the same techniques. The in situ gelation methods included the addition of an organic solution of either $PtBr_4$ or $(C_6H_5CN)_2PtCl_2$ to the alumina sol before gelation. The catalysts prepared by all the methods above were characterized in terms of Pt loading, Pt dispersion, and surface area.

2. Experimental

2.1. Preparation of nonhydrolytic amorphous alumina (NH)

$AlCl_3$ (Fluka, 99%), $Pr^{i}_{2}O$ (Riedel-deHaen, 99%), and CH_2Cl_2 (Carlo Erba, 99.8%) were added into a reactor under argon in a ratio of 1 g/1.6 ml/4.2 ml, respectively, as in [22]. After dissolution the reactor was immersed in an oil bath at 363 K for 24 h for gelation and aging. The average gelation time was 6.5 h with a standard deviation of 0.5 h. After aging the xerogels were dried at RT (293–298 K) under a mild vacuum of 25–40 N/m^2.

The fresh xerogels were calcined in dry air at 923 K for 5 h, to obtain the nonhydrolytic amorphous alumina. The heating rate was 40 K/h up to 673 K and then 70 K/h up to 923 K. The average SA of NH alumina was measured as 274 m^2/g.

2.2. Introduction of Pt

2.2.1. In situ introduction of Pt into NH alumina

2.2.1.1. Introduction with cis-bis(benzonitrile)platinum dichloride, $(C_6H_5CN)_2PtCl_2$ Two hours after the addition of the alumina precursors, as described above (before gelation), the sol was cooled and a solution of 0.02 g/ml of $(C_6H_5CN)_2PtCl_2$ in CH_2Cl_2 was added under argon. The amount of $(C_6H_5CN)_2PtCl_2$ solution added was equivalent to a final product of 1.0 wt.% Pt/Al_2O_3. The reactor was placed again in an oil bath at 363 K for an additional 22 h for gelation and aging. After aging the xerogels were dried at RT under a mild vacuum of 25–40 N/m^2. The catalyst was then calcined at various temperatures for 3–5 h. The 1.0 wt.% Pt content of the final catalysts was verified by dissolving the catalyst in concentrated HNO_3/HCl and analyzing the Pt concentration in the solution using a PE-SCIEX ELAN 6000 ICP-MS unit.

2.2.1.2. Introduction with $PtBr_4$ $PtBr_4$ did not dissolve in either $Pr^{i}_{2}O$ nor CH_2Cl_2, but was found to dissolve in a $Pr^{i}_{2}O/CH_2Cl_2$ mixture. However, the time required for the dissolution was several days. Therefore a stock solution of 0.05 g $PtBr_4$/1 ml $Pr^{i}_{2}O$/2.5 ml CH_2Cl_2 was used and the procedure was the same as for introduction by $(C_6H_5CN)_2PtCl_2$ except that $PtBr_4$ solution in $Pr^{i}_{2}O/CH_2Cl_2$ was used instead of $(C_6H_5CN)_2PtCl_2$ solution in CH_2Cl_2.

2.2.2. Introduction of Pt by impregnation

For the catalysts prepared by impregnation the above NH alumina and two commercial γ-Al_2O_3 of Alfa Aesar, termed below $\gamma1$ and $\gamma2$, were utilized, $\gamma1$ and $\gamma2$ possess SA of 170 and 227 m^2/g, respectively. Prior to the impregnation the NH and $\gamma2$ aluminas were ground to $\sim$ 50 µm ($\gamma1$ is in the form of $\sim$ 250 µm powder).

2.2.2.1. Impregnation by H_2PtCl_6 solution in water To each gram of Al_2O_3, 50 ml of a 100 or 200 µg Pt/ml, H_2PtCl_6 solution in water was added to obtain 0.5 or 1.0 wt.% Pt/Al_2Cl_3 catalysts, respectively. The mixture was stirred for 4 h, after which the catalyst was filtered. The catalyst was then dried at 383 K under vacuum and then calcined at 773 K for 3 h. The liquid phase was analyzed for Pt traces by a UNICAM. UV/V is spectrometer operated at 262 nm or with a VARIAN 400 atomic absorption instrument.

2.2.2.2. Impregnation by Pt(acac)$_2$ solution in toluene The alumina was initially dehydrated under dry air at 773 K and cooled under the same atmosphere. The alumina was then added to 125 or 250 µg Pt/ml, Pt(acac)$_2$ solution in toluene in a ratio of 40 ml/g alumina to yield 0.5 or 1.0 wt.% Pt/Al_2O_3 catalysts, respectively. The mixture was stirred for 4 h, after which the catalyst was filtered. The catalyst was then dried at 383 K under vacuum and then calcined at

773 K for 3 h. The liquid phase was analyzed for Pt traces by a VARIAN 400 atomic absorption instrument. In order to avoid interference caused by toluene, before the atomic absorption the toluene was exchanged with methyl isobutyl ketone.

2.3. Characterization of the catalysts

Thermal behavior of the xerogels was studied by DTA/TGA measured in a Setaram TG-92 unit, in flowing air, with a heating rate of 5 K/min, and the composition of the effluent gas was detected using a mass spectrometer (Balzers Thermostar GSD300T).

BET specific surface areas were determined by nitrogen desorption using a Quantachrome Monosorb. XRD patterns were recorded using a Siemens 5000 instrument employing Cu-K_α radiation. The catalysts were observed by a JEOL STEM FX-2000 operated at 200 kV and equipped with a LINK AN 10000 EDS system. TPR and H_2 pulse chemisorptions measurements were held on a Zeton Altamira AMI200 instrument. The TPR was held using 10% H_2/Ar gas and a heating rate of 10 K/min up to 673 K. For the H_2 pulse chemisorptions, samples which were reduced by 10% H_2/Ar gas at 673 K and then saturated by oxygen using a 10% O_2/He stream at 308 K were used. The number of 10% H_2/Ar pulses into Ar which were consumed by the sample was recorded. The surface reaction [41]

$$\text{Pt–O} + \tfrac{3}{2}H_2 \rightarrow \text{Pt–H} + H_2O$$

was assumed to calculate the Pt dispersion.

3. Results and discussion

3.1. Catalysts prepared by in situ introduction of Pt into NH alumina

3.1.1. Effect of in situ Pt introduction into NH alumina on thermal behavior

The thermal behavior of the fresh xerogel with and without the Pt upon treatment in air was examined by TGA/DTA, and is shown in Fig. 1. For the xerogel without Pt (see a and d), below 470 K the weight loss was due to evaporation of organic residues from the xerogel. This region is accompanied by a small endotherm observed in the DTA (d). For the Pt-free xerogels, the weight loss between 470 and 870 K is due to oxidation of the organic residues. This segment is accompanied by two exothermic peaks observed in the DTA with maximums at 570 and 770 K. The oxidation of the organic residues is completed by ~ 870 K as seen by the TGA and DTA curves. At a higher temperature of ~ 1070 K an exothermic peak is observed in the DTA. This peak is attributed to crystallization into γ-Al_2O_3. The main difference between the TGA/DTA patterns of fresh xerogels with in situ introduction of Pt (b, c, e, f) from the TGA/DTA curves of fresh xerogels without Pt is in the sharp ending of the organic residues burnout at lower temperatures of 740 and 770 K using $PtBr_4$ and $(C_6H_5CN)_2PtCl_2$ solutions, respectively. In [42] the lower burning temperature of organic residues of co-gelled Pd/SiO_2 vs the higher burning temperature of Pd-free samples was explained by the oxidation power of Pd. TGAs of $PtBr_4$ and $(C_6H_5CN)_2PtCl_2$ in air (not shown) revealed that the decomposition to metallic Pt is over at 748 and 763 K, respectively. The mechanism of this platinum reduction is not clear and the Pt complex fixed to the fresh xerogel may be different from the original complex. However, it is logical to assume that at temperatures a little lower than 773 K, the Pt in the alumina is converted to the metallic state, and then catalyzes the burnout of the organic and coke residues at much lower temperatures than in the xerogels without Pt. This explanation, which is based on formation of metallic Pt, is supported by the fact that the XRD of samples in which Pt was introduced in situ, and then calcined in air at 873 K, revealed the presence of crystalline Pt (Fig. 2). The intensity of the reduction peaks observed in the H_2 TPR patterns of catalysts which were previously calcined at 873 K (not shown) correspond to ~ 25% reduction, which also suggests that part of the Pt was converted to the metallic state during the calcination in air.

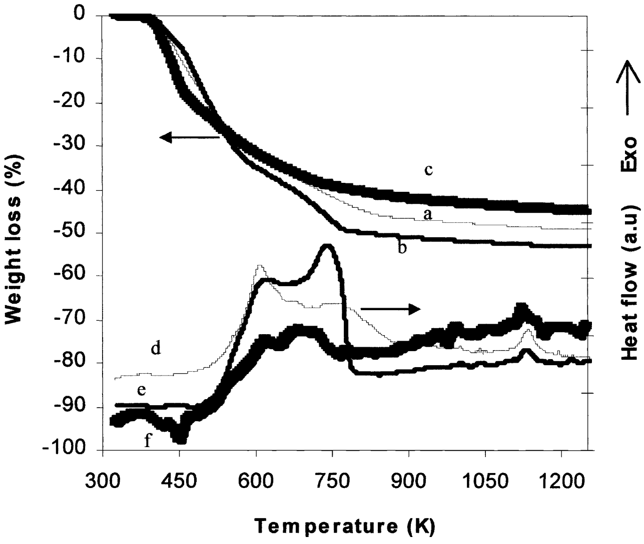

Fig. 1. TGA and DTA curves in the range 300–1250 K for pure NH-alumina xerogel (a, d), NH alumina with in situ $(C_6H_5CN)_2PtCl_2$ xerogel (b, e), and NH alumina with in situ $PtBr_4$ xerogel (c, f). Heatings were done in air at 5 K/min.

3.1.2. SA of calcined catalysts

The average SA of catalysts calcined at 773 and 873 K in air is summarized in Table 1. As seen in Table 1, there is a significant decrease in SA for the pure NH alumina samples from 420 to 320 m^2/g when the calcination temperature is increased from 773 to 873 K. For the platinum-containing samples the SA remains constant in the same temperature range (~ 330 m^2/g), similarly to the SA of pure NH alumina calcined at 873 K. The lower SA of the Pt-containing

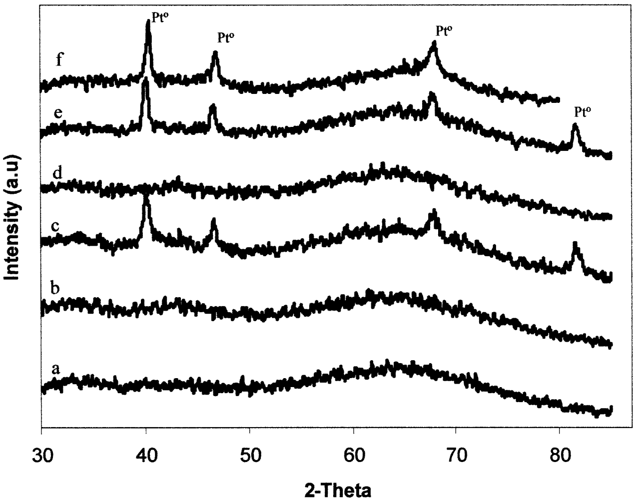

Fig. 2. XRD patterns of NH alumina with in situ, introduction of $(C_6H_5CN)_2PtCl_2$ and after heat treatments at (a) 773 K air; (b) 773 K air; 673 K H_2; (c) 873 K air, and of NH alumina with in situ introduction of $PtBr_4$ and after heat treatments at (d) 773 K air, H_2 673 K; (e) 873 K air; (f) 1023 K air.

samples compared to the NH alumina after calcination at 773 K, may be due to differences caused by the addition of the organic solvents and/or the Pt precursor during gelation, which causes the evolution of different microstructures. Another possible explanation for the reduced SA of the Pt-containing samples is the catalyzed organic burn-off. The catalyzed burn-off causes a local increase in the temperature within the catalyst pellets, which is observed in the DTA curves (Fig. 1 e, f). This local increased temperature results in higher actual calcination temperature and therefore causes lower SA.

3.1.3. The effect of thermal treatment on Pt accessibility and dispersion

The effect of heat treatments on Pt dispersion (and particle size) was examined by XRD (Fig. 2), by TEM (Fig. 3), and by H_2 pulse chemisorption (Table 1). In samples which were calcined under air at temperatures lower then 773 K the Pt is well dispersed, as can be seen from the absence of Pt peaks from the XRD pattern of the H_2 reduced sample (Fig. 2 b, d), which suggest that Pt crystallites are smaller than 5 nm [43]. In the TEM micrographs of samples calcined at 773 K (not shown) Pt particles are not detectable, which is consistent with the XRD data. In spite of the fact that TEM and the XRD pattern suggest that the Pt is well dispersed, the Pt might be buried as very small crystallites within the alumina matrix. These small crystallites, which will not contribute to the catalytic activity, due to inaccessibility of the gas phase, are not observed in the TEM or in the XRD pattern. However, H_2 pulse chemisorption over reduced samples, which is only sensitive to surface atoms, shows Pt dispersion of ca. 30%, which means that significant portion of the Pt atoms are exposed at the surface. We therefore conclude that even if the Pt precursor is buried within the xerogel during the gelation process, a major portion of Pt atoms are accessible surface atoms after thermal treatment of the catalyst.

Table 1
Surface area and Pt dispersion—in situ introduction of Pt

Pt precursor	Surface area (m^2/g)		Pt dispersion from pulse chemisorption (%)	
	773 K calcination	873 K calcination	773 K calcination	873 K calcination
None (pure Al_2O_3)	420	320	–	–
$PtBr_4$	320	330	32	13
$(C_6H_5CN)_2PtCl_2$	350	330	32	7

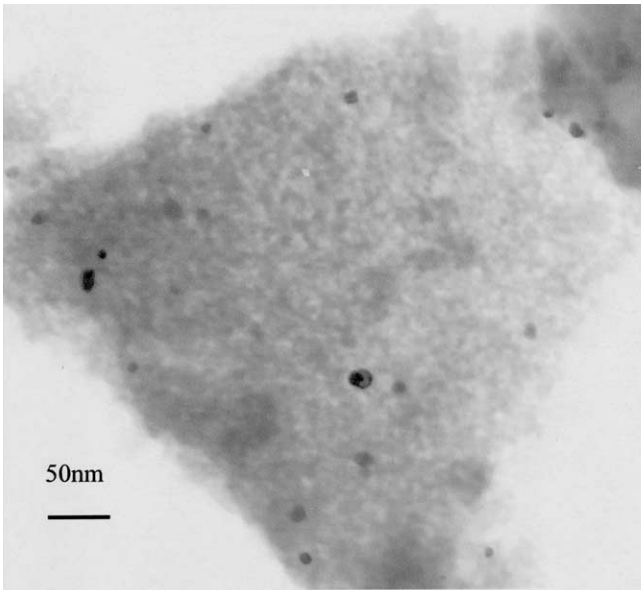

Fig. 3. TEM micrographs of NH alumina with in situ introduction of $(C_6H_5CN)_2PtCl_2$ after heat treatment at 873 K under air.

Upon higher temperature treatment in air ($T = 873$ K), there is extensive sintering of Pt, as can be seen by the appearance of Pt peaks in the XRD pattern (Fig. 2 c, e). From the width of the 2θ peak centered at $\sim 40°$, and using Scherrer's equation [44] and assuming spherical shape of Pt crystals, the average Pt size is ~ 25 nm. This particle size is slightly larger than the Pt particles observed in the TEM micrographs (Fig. 3) as dark features of 10–20 nm. The dark features in the TEM micrographs were proved to be Pt by EDS in the STEM mode. The larger particle size obtained by XRLBA is probably due to the fact that the XRD line-broadening is a volume-average particle size, which is larger than the sample mean diameter. Further H_2 treatment, at 723 K, of samples previously calcined under air at $T \geqslant 873$ K did not significantly affect the intensity of the Pt peaks nor the line broadening of the Pt peaks, which suggests that the sintering into large Pt crystals occurs during the high-temperature air treatment and not during subsequent H_2 treatment. Increasing the air calcination temperature to 1023 K resulted in increased intensity of the Pt peaks (almost double the intensity obtained at 873 K) and a further increase of the mean particle size to ∼ 30 nm. The increase in the Pt peaks' intensity with increased calcination temperature suggests that not all of the Pt in samples calcined at 873 K is in the form of large metallic Pt crystals, which are detected by XRD. The Pt which was not detected by XRD might be in the form of small crystals or of a noncrystalline species. Upon increased temperature air treatment (1023 K), this noncrystalline/well-dispersed platinum sinters into large Pt crystals. Support for the existence of small Pt crystals not detected by XRD after 873 K calcination comes from comparing the dispersions obtained by XRD to the dispersions obtained by the pulse chemisorption. The mean particle size of 25 nm obtained by XRD corresponds to ∼ 4% dispersion. The dispersions obtained by pulse chemisorption (Table 1) are, however, higher (7–13%), which suggests the existence of small Pt crystals which are not detected by XRD but do contribute most of the Pt dispersion.

3.2. Catalysts impregnated by $Pt(acac)_2$ solution in toluene

3.2.1. Pt uptake during impregnation

The Pt uptake by the catalyst was calculated by a mass balance on the Pt content in the liquid phase (detected by atomic absorption) before and after contact with the alumina and is shown in Table 2. For catalysts impregnated with a solution containing Pt in amounts adequate to 0.5 wt.% Pt/Al_2O_3, almost all of the Pt is fixed on the alumina surface. According to [29,30] this Pt is fixed by the following surface reaction:

$$\text{Surface–OH} + Pt(acac)_2 \Longleftrightarrow \text{surface–O–Pt(acac)} + Acac_{\text{adsorbed}}.$$

However, for catalysts impregnated with a solution containing Pt in amounts adequate to 1.0 wt.% Pt/Al_2O_3, there is a significant amount of Pt residue in the solution after contact with $\gamma 1$, $\gamma 2$ aluminas, while the NH alumina practically fixes all of the Pt. This means that the NH alumina possesses more sites that can adsorb the $Pt(acac)_2$ complex. The $Pt(acac)_2$ fixation reaction with the support is an acidic reaction. The origin of the higher number of fixation sites on the NH alumina may be the high chlorine content in the NH alumina, which increases the support acidity, or the higher SA of the NH alumina. The Pt loading NH > $\gamma 2$ > $\gamma 1$ is in the same order as the SA of these aluminas, which is in line with the second explanation.

Table 2
SA, Pt uptake and dispersion—impregnation by $Pt(acac)_2$/toluene

Alumina	Amount of Pt in initial solution (wt.%)	Actual Pt loading (wt.%)	Surface area[a] (m^2/g)	Pt dispersion from pulse chemisorption (%)[b]
NH	0.5	0.46	267	49
	1.0	0.96	252	28
$\gamma 1$	0.5	0.41	180	37
	1.0	0.57	176	37
$\gamma 2$	0.5	0.45	219	43
	1.0	0.71	213	39

[a] After calcination at 773 K.

[b] Based on actual Pt loading.

3.2.2. SA

After calcination at 773 K all catalysts regained the surface area of the original alumina supports; i.e., the aluminas do not undergo morphological changes during contact with the toluenic solution of $Pt(acac)_2$. As will be discussed later, the SA of the NH alumina changes significantly during impregnation with aqueous solution.

3.2.3. Pt dispersion

The Pt dispersion was evaluated after calcination at 773 K. In the TEM micrographs no Pt particles were observed, which is consistent with the good Pt dispersions measured by the H_2 pulse chemisorptions (Table 2). Increasing the Pt loading did not affect the Pt dispersion for the $\gamma 1$, $\gamma 2$ catalysts. However, for the NH alumina, there is a decrease in the Pt dispersion with increase of Pt uptake. This may suggest that the enhanced Pt adsorption on the NH alumina is on weak adsorption sites, which release the Pt rather readily upon thermal treatment, resulting in sintering and lower Pt dispersion.

3.3. Catalysts impregnated by H_2PtCl_6 solution in water

3.3.1. Pt uptake during impregnation

As in the previous section, the Pt uptake by the catalyst was calculated by a mass balance on the Pt content in the liquid phase (detected by atomic absorption or by spectrophotometry) before and after contact with the alumina and is shown in Table 3. For all three aluminas and for the nominal loading of 0.5 and 1.0 wt.%, more than 98% uptake of the Pt from the water was obtained. The nature of Pt uptake from aqueous H_2PtCl_6 solution, although studied for many decades, is not fully understood [16–21], however, the full Pt uptake for all aluminas may suggest that the fixation of Pt is of the same nature for the NH amorphous alumina and the γ-aluminas.

3.3.2. SA

After calcination in air at 773 K the catalysts obtained from impregnation of the commercial $\gamma 1$, $\gamma 2$ aluminas regained the original surface area (Table 3). However, the catalysts obtained by impregnation of the NH amorphous alumina followed by calcination at 773 K had a significantly lower surface area (175 m^2/g) than the original NH support (274 m^2/g). In a previous study [22], it was been found that upon contact of the NH amorphous alumina with water, at RT, for periods of up to several days and subsequent thermal treatment the SA of the alumina decreases. The suggested explanation for the decrease in SA was a condensation reaction, which may block some of the pores, resulting in lower SA.

Table 3
SA, Pt uptake and dispersion—impregnation by H_2PtCl_6/water

Alumina	Amount of Pt in initial solution (wt.%)	Actual Pt loading (wt.%)	Surface area[a] (m^2/g)	Pt dispersion from pulse chemisorption (%)
NH	0.5	0.5	177	15
	1.0	0.99	173	21
$\gamma 1$	0.5	0.5	189	45
	1.0	0.99	178	39
$\gamma 2$	0.5	0.49	227	41
	1.0	0.99	213	39

[a] After calcination at 773 K.

3.3.3. Pt dispersion

The Pt dispersion was evaluated after calcination at 773 K. In the TEM micrographs no Pt particles were observed and in the XRD pattern of these catalysts after reduction in H_2 at 673 K no Pt peaks are observed, which is consistent with the good Pt dispersions measured by the H_2 pulse chemisorptions for the $\gamma 1$, $\gamma 2$ aluminas (Table 3). For the NH alumina, however, the $\sim 20\%$ dispersion corresponds to crystallites of average size 5–6 nm, which are expected to be observed in TEM and to cause the appearance of wide Pt peaks in the XRD. However, no Pt crystals were observed in the TEM, and no traces of Pt peaks were observed in the XRD pattern of the Pt/NH-alumina samples. We therefore conclude that the Pt is spread as small species (not detectable by TEM or XRD), which are partially buried within the alumina matrix. The mechanisms by which the Pt may be buried within the alumina are:

(a) The condensation reaction, described above, which may block some of the pores.
(b) Upon contact with water the NH amorphous alumina undergoes a dissolution–reprecipitation process [22]. At RT this process takes up to several weeks. The adsorption of Pt from the water is over at a much shorter time. We therefore suggest that after the Pt complex is fixed to the alumina from the water it may be buried by the dissolution–reprecipitation of the NH alumina. As a result of this process the Pt is spread as small species partially buried within the alumina matrix.

4. Summary

The synthesis of Pt/NH–amorphous-alumina catalysts by (a) in situ introduction of $PtBr_4$ or $(C_6H_5CN)_2PtCl_2$, during gelation of the NH alumina, (b) by impregnation with $Pt(acac)_2$ solution in toluene, or (c) by impregnation with H_2PtCl_6 solution in water was investigated. Pt/γ-alumina catalysts prepared by the same impregnation methods were used as a reference for comparison. The main findings are:

(1) About 30% of the Pt atoms of Pt/NH–amorphous-alumina catalysts prepared by in situ introduction of $PtBr_4$ or $(C_6H_5CN)_2PtCl_2$, are exposed at the surface after calcination at 773 K. Increasing the calcination temperature to 873 K results in sintering of part of the Pt to crystals of an average size of ~ 20 nm.
(2) The NH alumina fixes Pt from $Pt(acac)_2$ solution in toluene more readily than the γ-aluminas. Upon calcination at 773 K of 0.5 wt.% Pt/alumina catalysts the obtained Pt dispersions are $\sim 50\%$ for the NH alumina and $\sim 40\%$ for the γ-aluminas. Increasing the Pt loading does not affect the dispersion obtained with both γ-aluminas, whereas the sintering of the Pt leading to a lower dispersion is more pronounced for the NH alumina.
(3) The NH and the γ aluminas fixe Pt from aqueous H_2PtCl_6 solution. Complete Pt uptake from the water was obtained for the 1.0 wt.% catalysts. However, the dispersion obtained after calcination at 773 K of the Pt/NH-alumina ($\sim 20\%$) is inferior to the dispersion obtained with γ-aluminas ($\sim 40\%$). The NH alumina also suffers a decrease in SA upon contact with water. These findings are explained by a condensation reaction, which may block some of the pores, and by the dissolution–reprecipitation process of the NH alumina which buries the Pt.

The effect of the synthesis method and the type of alumina used on catalytic activity is currently under investigation.

Acknowledgments

The authors thank the Israel Science Foundation, the Technion Grand Water Institute, the Technion Catalysis Project, and the Center for Adsorption in Science of the Ministry of Immigrant Absorption (under the framework of the KAMEA program) for their support. In addition, the authors thank Dr. Michael Reisner for help in X-ray measurements.

References

[1] R.K. Oberlander, in: B.E. Leach (Ed.), Applied Industrial Catalysis, Vol. 3, Academic Press, London, 1984, p. 63.
[2] B.E. Yoldas, J. Appl. Chem. Biotechnol. 23 (1973) 803.
[3] C.J. Brinker, G.W. Scherer, Sol–Gel Science: The Physics and Chemistry of Sol–Gel Processing, Academic Press, New York, 1990.
[4] Y. De Hazan, G.E. Shter, Y. Cohen, C. Rottman, D. Avnir, G.S. Grader, J. Sol–Gel Sci. Technol. 14 (3) (1999) 233.
[5] G.S. Grader, Y. De Hazan, D.B. Zhivotovskii, G.E. Shter, J. Sol–Gel Sci. Technol. 10 (1997) 127.
[6] S. Acosta, R. Corriu, D. Leclercq, P.H. Mutin, A. Vioux, J. Sol–Gel Sci. Technol. 2 (1994) 25.
[7] S. Acosta, P. Arnal, R.J.P. Corriu, D. Leclercq, P.H. Mutin, A. Vioux, in: Better Ceramics through Chemistry VI, in: Mater. Res. Soc. Symp. Proc., Vol. 346, 1994, p. 43.
[8] S. Acosta, R.J.P. Corriu, D. Leclercq, P. Lefevre, P.H. Mutin, A. Vioux, J. Non-Cryst. Solids 170 (1994) 234.

[9] M. Andrianainarivelo, R.J.P. Corriu, D. Leclercq, P.H. Mutin, A. Vioux, J. Mater. Chem. 7 (2) (1997) 279.

[10] M. Andrianainarivelo, R.J.P. Corriu, D. Leclercq, P.H. Mutin, A. Vioux, Chem. Mater. 9 (5) (1997) 1098.

[11] M. Andrianainarivelo, R. Corriu, D. Leclercq, P.H. Mutin, A. Vioux, J. Mater. Chem. 6 (10) (1996) 1665.

[12] G.E. Costa, N.S. Figoli, M.R. Sad, G.T.O. Zwiener, L.M. Krasnogor, J.M. Parera, React. Kinet. Catal. Lett. 20 (12) (1982) 171.

[13] J. Hancsok, G. Gardos, J. Perger, Hung. J. Ind. Chem. 15 (3) (1987) 309.

[14] J.P. Boitaux, J.M. Deves, B. Didillon, C.R. Marcilly, in: G.J. Antos, A.M. Aitani, J.M. Parera (Eds.), Catalytic Naphtha Reforming Science and Technology, Dekker, New York, 1995, p. 79.

[15] D. Maret, G.M. Pajonk, S.J. Teichner, in: G.M. Pajonk, S.J. Teichner, G.E. Germain (Eds.), Spillover of Adsorbed Species, Elsevier, Amsterdam, 1983, p. 215.

[16] R.D. Gonzalez, H. Miura, Catal. Rev. Sci. Eng. 36 (1) (1994) 145.

[17] J.P. Brunelle, Pure Appl. Chem. 50 (1978) 1211.

[18] J.C. Summers, S.A. Ausen, J. Catal. 52 (1978) 445.

[19] J.R. Regalbuto, A. Navada, S. Shadid, M.L. Bricker, Q. Chen, J. Catal. 184 (1999) 335.

[20] B.N. Shelimov, J.F. Lambert, M. Che, B. Didillon, J. Mol. Catal. 158 (2000) 91.

[21] B. Shelimov, J.F. Lambert, M. Che, B. Didillon, J. Am. Chem. Soc. 121 (3) (1999) 545.

[22] G.S. Grader, G.E. Shter, D. Avnir, H. Frenkel, D. Sclar, A. Dolev, J. Sol–Gel Sci. Technol. 21 (3) (2001) 157.

[23] F. Abbattista, S. Delmastro, G. Gozzelino, D. Mazza, M. Vallino, G. Busca, V. Lorenzelli, G. Ramis, J. Catal. 117 (1989) 42.

[24] B. Coq, E. Crabb, M. Warawdekar, G.C. Bond, J.C. Slaa, S. Galvagno, L. Mercadante, J.G. Ruiz, M.C.S. Sierra, J. Mol. Catal. 92 (1) (1994) 107.

[25] C.G. Walter, B. Coq, F. Figueras, M. Boulet, Appl. Catal. A 133 (1) (1995) 95.

[26] L.C. de Menorval, A. Chaqroune, B. Coq, F. Figueras, J. Chem. Soc. Faraday Trans. 93 (20) (1997) 3715.

[27] Z. Gandao, B. Coq, L.C. de Menorval, D. Tichit, Appl. Catal. A 147 (2) (1996) 395.

[28] P. Reyes, G. Pecchi, M. Morales, J.L.G. Fierro, Appl. Catal. A 163 (1997) 145.

[29] J. Berdala, E. Freund, J.P. Lynch, J. Phys. Colloq. C 8 (1) (1986) C8/265.

[30] J.P. Boitiaux, J. Cosyns, S. Vasudevan, in: G. Poncelet, P. Grange, P.A. Jacobs (Eds.), Preparation of Catalysts III, Elsevier, Amsterdam, 1983, p. 123.

[31] B. Coq, A. Tijani, F. Figueras, J. Mol. Catal. 71 (3) (1992) 317.

[32] B. Coq, A. Chaqroune, F. Figueras, B. Nciri, Appl. Catal. A 82 (2) (1992) 231.

[33] T. Lopez, M. Asomoza, P. Bosch, E.G. Figueroa, R. Gomez, J. Catal. 138 (1992) 463.

[34] T. Lopez, P. Bosch, M. Moran, R. Gomez, J. Phys. Chem. 97 (1993) 1671.

[35] T. Lopez, R. Gomez, J. Navarrete, R.D. Gonzalez, J. Mater. Synth. Process. 2 (1994) 305.

[36] O. Bokhimi, A. Aceves, O. Novaro, T. Lopez, R. Gomez, J. Phys. Chem. 99 (1995) 14403.

[37] E. Sanchez, T. Lopez, R. Gomez, O. Bokhimi, A. Morales, O. Novaro, J. Solid State Chem. 122 (1996) 309.

[38] S. Castillo, M.M. Pineda, V. Molina, R. Gomez, T. Lopez, Appl. Catal. B 15 (1998) 203.

[39] I.H. Cho, S.B. Park, S.J. Cho, R. Ryoo, J. Catal. 173 (1998) 295.

[40] C. Gorsmann, U. Schubert, J. Leyrer, E. Lox, Mater. Res. Soc. Symp. Proc. 435 (1996) 625.

[41] J.E. Benson, M. Boudart, J. Catal 4 (1965) 704.

[42] B. Heinrichs, F. Noville, J.P. Pirard, J. Catal. 170 (1997) 366.

[43] T.A. Dorling, R.L. Moss, J. Catal. 7 (1967) 378.

[44] J.L. Lemaitre, P.G. Menon, F. Delannay, in: F. Dellanay (Ed.), Characterization of Heterogeneous Catalysts, Dekker, New York, 1984, p. 299.